

Article

Study on Vibration Friction Reducing Mechanism of Materials

Yunnan Teng *, Quan Wen, Liyang Xie and Bangchun Wen

Department of Mechanical Engineering and Automation, Northeastern University, Shenyang 110819, China

* Correspondence: ynteng@me.neu.edu.cn

Abstract: Friction has a vital role in studying materials' and systems' behavior. The friction between two objects and the inner friction of materials under the condition of vibration usually can present different characteristics. These characteristics are different from the conventional conditions. It is shown in practice that vibration can reduce the friction coefficient and friction force between two objects. Vibration can lighten abrasion of objects and reduce energy consumption. All of these can give great efficiency, but, until now, the vibration friction-reducing mechanism has not been fully revealed. In this manuscript, the friction-reducing mechanism of materials under arbitrary vibration forces is investigated. The results show that the effective friction coefficient of materials under arbitrary vibration forces is always the minimum. The relationship between the effective friction coefficient and the negative gradient is investigated in this research. When the vibration force direction projects are in the first and the third quadrants, the negative gradient of the effective friction coefficient gets larger slowly, and then it becomes stable. When the vibration force direction projects are in the second and the fourth quadrants, the negative gradient of the effective friction coefficient decays to zero at the initial stage and then increases rapidly.

Keywords: vibration; friction; effective friction coefficient; negative gradient

MSC: 74H45



Citation: Teng, Y.; Wen, Q.; Xie, L.; Wen, B. Study on Vibration Friction Reducing Mechanism of Materials. *Mathematics* **2022**, *10*, 3529. <https://doi.org/10.3390/math10193529>

Academic Editors: Maria Luminița Scutaru and Catalin I. Pruncu

Received: 28 August 2022
Accepted: 26 September 2022
Published: 28 September 2022

Publisher's Note: MDPI stays neutral with regard to jurisdictional claims in published maps and institutional affiliations.



Copyright: © 2022 by the authors. Licensee MDPI, Basel, Switzerland. This article is an open access article distributed under the terms and conditions of the Creative Commons Attribution (CC BY) license (<https://creativecommons.org/licenses/by/4.0/>).

1. Introduction

Vibration is common in engineering practice and daily life, and it is the main content in the study of vibration friction mechanics. We are always in a vibration environment, such as the vibration of houses and bridges, the vibration of machine tools, the vibration of engines, and the vibration of road rollers and sinking and pulling machines. In the progress of science and engineering, a lot of mechanical equipment are moving towards high speed, high precision, and miniaturization [1,2]. Research on vibration is becoming more and more important. It is necessary to master vibration law and the transmission path of the interface so as to reasonably use or suppress vibration. One of the most important problems with vibration is the friction between interfaces. It is the key to improving the reliability and life of machinery and equipment, and its economic significance is very clear. In industry, generally in this case, the main reason leading to the failure of machines is not damage of the components of the machine itself but the wear of the contact interface of various parts under the action of fretting or sliding friction [3–8]. As one of the most fundamental physical phenomena, friction is the most common phenomenon, and vibration friction usually happens in mechanical systems [9–12]. Many researchers have focused on the relationships between vibration and friction. On the basis of oil film dynamic pressure lubrication and an elastic contact model of the asperities, Bao et al. set up a kinematic coupling model of the rotation-axial engagement process according to friction elements and gave the engagement characteristics of the multi-disc wet friction clutch [13]. Marques et al. studied several friction force models dealing with different friction phenomena in the research of multibody system dynamics [14]. To study the random stick-slip vibration of duffing systems of dry friction, a numerical approximate solution was performed by Jin et al. [15].

Some researchers performed experimental validation and investigations of vibration friction systems [16–18]. Sun et al. analyzed the friction coefficient based on the recurrence plots and proposed a new method to identify the running-in state of the friction pair [19,20]. Many nonlinear phenomena were presented in engineering of the discontinuities introduced by friction in the governing equations [21–23]. In engineering practice, friction between the contact bodies can cause lots of undesirable effects on the system, such as frictional chatter [24], wear in friction-induced vibrations [25,26], and reduction characteristics of silicon [27]. The natural frequencies and damped forced vibrations were investigated by Safaei for an improved and lightweight sandwich plate of a periodic load in a limited time [28]. Doan et al. analyzed the free vibration and static buckling of flexoelectric variable thickness nanoplates. To emphasize the affection of flexoelectricity in free vibration and static buckling of the nanoplates, a variety of parameter studies was conducted [29]. A nonlinear static bending study of microplates resting on imperfect Pasternak elastic foundations was carried out by Thai Dung et al. By the improved couple stress theory and finite element methods, the nonlinear finite element formulations were performed [30]. For illustration as a stationary process with white noise, the vibration response of beams in the condition of random load was studied by Nguyen et al. To predict the fundamental frequencies of the structures, the artificial neural network (ANN) model was presented [31]. The dynamic problem for the moment theory of elasticity related to the finite length crack in normal stress conditions on the banks was demoted to a series of displacement and rotation integral equations in [32], which were performed mathematically. Moreover, in [33], the dynamic problems related to micro-polar elastic bodies were carried out by an eigenvalues technique. Lai Thanh Tuan et al. devised and performed numerical and analytical solutions for problems in two dimensions, including the spreading of unsteady axisymmetric boundary disturbances of a “non-classical” elastic medium of spherical boundaries [34]. Recently, based on a serious of methodologies, many researchers have performed numerous studies on the computation of plate and shell structures. Many beneficial discoveries were made [35–39].

However, several problems for vibration friction in the case of arbitrary vibration working environments have not yet been sufficiently studied, including the effective coefficient of dynamic friction and the friction mechanism in arbitrary vibration of materials and the negative gradient of friction.

The purpose of this paper is to present the friction-reducing mechanism of materials under arbitrary vibration forces. Due to limitations associated with the negative gradient of the effective friction coefficient and the effective friction coefficient in arbitrary vibration working environments, the vibration friction characteristics of materials have not been thoroughly explained. Based on the effective coefficient of dynamic friction and the friction mechanism in arbitrary vibration of materials, the effective friction coefficient was deduced in this research, and the negative gradient of friction was also discussed.

The main body of this paper is split into four sections. The material model is presented in Section 2. The effective coefficient of friction is studied in Section 3. The negative gradient of the effective friction coefficient is given in Section 4. In Section 5, important conclusions are summarized.

2. Model of Material

It is a very common phenomenon that materials always vibrate under the vibration condition in engineering. In the last century, some researchers proposed the concept of effective friction coefficient from the perspective of breaking static conditions by using pure mechanical methods [14,17]. In this paper, the concept of effective friction coefficient is used to study the friction reduction effect of vibration under three conditions: that the vibration direction is parallel to the force, the vibration direction is parallel to the normal pressure, and the vibration direction is perpendicular to the force and the normal pressure. Then, on the basis of these three conditions, the effective friction coefficient formula of vibration in an arbitrary direction is further derived. It is proved that vibration can reduce friction. The

influence and control of vibration parameters on friction reduction are explained by the change in effective friction coefficient reduction rate in this paper.

Firstly, the model is established in a Cartesian coordinate system. This is shown in Figure 1. The effective friction coefficient is f^* ; f_1 is the coefficient of the maximum static friction between the material and the surface; N is the normal compression force (opposite paralleled axis Z); Q is the tension force (paralleled axis X); F_0 is the amplitude of the force $F(t)$; $F(t) = F_0 \sin(\omega t + \phi)$; Q_{min} is the minimum force to move the material. P is the gravity force, $P = mg$.

$$Q_{min} = (N + mg)f_1 - F_0 = f_1(N + mg) \left(1 - \frac{F_0}{f_1(N + mg)}\right), \tag{1}$$

$$f^* = \frac{Q_{min}}{N + mg} = f_1 \left(1 - \frac{F_0}{f_1(N + mg)}\right). \tag{2}$$

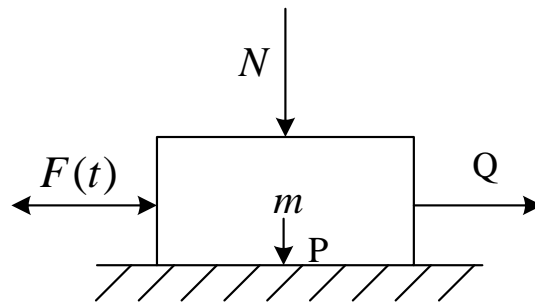


Figure 1. The vibration model of parallel force.

This is the effective friction coefficient formula under the condition that the vibration and the force direction are parallel. Since $\frac{F_0}{f_1(N+mg)} > 0$, the effective friction coefficient under vibration is less than the coefficient of the max static friction f_1 ; thus, the effective friction under vibration is reduced.

When the vibration direction is parallel to the normal pressure, the material model is shown in Figure 2.

$$Q_{min} = (N + mg - F_0)f_1 = f_1(N + mg) \left(1 - \frac{F_0}{N + mg}\right), \tag{3}$$

$$f^* = \frac{Q_{min}}{N + mg} = f_1 \left(1 - \frac{F_0}{N + mg}\right). \tag{4}$$

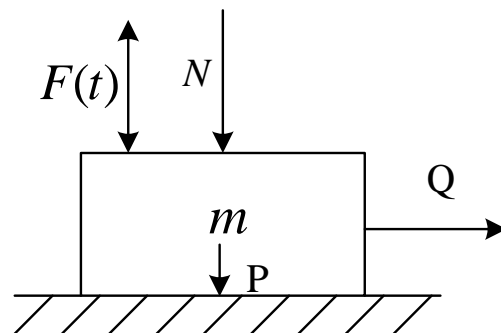


Figure 2. The vibration model of vertical force.

When the vibration direction is perpendicular to the force and the normal pressure, the material model is shown in Figure 3.

$$Q_{min} = \sqrt{(f_1(N + mg))^2 - F_0^2} = f_1(N + mg)\sqrt{1 - \left(\frac{F_0}{f_1(N + mg)}\right)^2}, \tag{5}$$

$$f^* = \frac{Q_{min}}{N + mg} = f_1\sqrt{1 - \left(\frac{F_0}{f_1A}\right)^2}. \tag{6}$$

where $A = N + mg$, and P is the gravity force; $P = mg$.

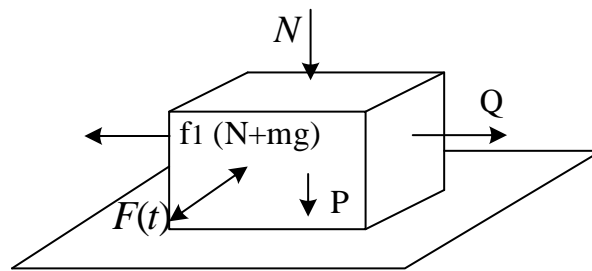


Figure 3. The model of vibration vertical to the friction and the normal pressure.

Similarly, the effective friction under vibration is reduced in these conditions. Then, on the basis of these three conditions, the effective friction coefficient formula of vibration in an arbitrary direction is further derived. Arbitrary vibration force can be seen as three components, and the effective friction coefficient under the arbitrary time-varying external forces is one of the critical characters to show the nonlinear dynamic characteristics of the system. Herein, it is studied in different conditions, respectively.

Firstly, the model is established in a Cartesian coordinate system, as shown in Figure 4. Next, m is the mass; f_1 is the coefficient of the maximum static friction between the material and the surface; N is the normal compression force (opposite paralleled axis Z); Q is the tension force (paralleled axis X); F_0 is the amplitude of the force $F(t)$; $F(t) = F_0 \sin(\omega t + \phi)$ is the arbitrary time-varying external forces, and its vectors are α, β, γ . P is the gravity force, $P = mg$. Then, the arbitrary time-varying external forces in different conditions are discussed separately.

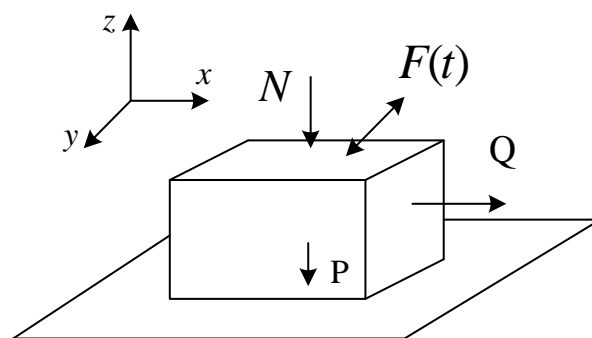


Figure 4. Model of the vibratory material under arbitrary vibration.

3. Effective Coefficient of Friction f^*

When the arbitrary time-varying external force projects are in the first and the third quadrants of the xz plane (including the limit boundary: projection in the axis z), the

maximum synthetic tension and the minimum compression are obtained, as shown in Figure 5. Herein, the force Q comes to Q_{min} and yields

$$(Q_{min} + F_0 \cos \alpha)^2 + (F_0 \cos \beta)^2 = (f_1(N + mg - F_0 \cos \gamma))^2, \tag{7}$$

where Q_{min} is the minimum force to move the material.

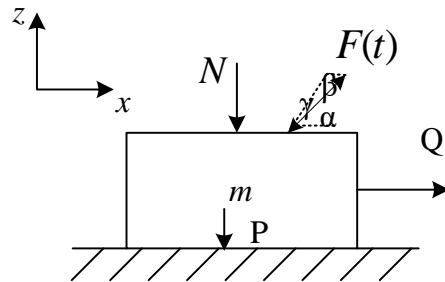


Figure 5. Vibration force projects in the first and the third quadrants.

Then, there is

$$f^* = f_1 \left(\sqrt{\left(1 - \frac{F_0 \cos \gamma}{N + mg}\right)^2 - \left(\frac{F_0 \cos \beta}{f_1(N + mg)}\right)^2} - \frac{F_0 \cos \alpha}{f_1(N + mg)} \right), \tag{8}$$

where f^* is the effective coefficient of friction.

Here, supposing $f^* \geq f_1$, there is

$$\sqrt{\left(1 - \frac{F_0 \cos \gamma}{N + mg}\right)^2 - \left(\frac{F_0 \cos \beta}{f_1(N + mg)}\right)^2} - \frac{F_0 \cos \alpha}{f_1(N + mg)} \geq 1. \tag{9}$$

$A = N + mg$, then there is

$$\left(1 - \frac{F_0 \cos \gamma}{A}\right)^2 - \left(\frac{F_0 \cos \beta}{f_1 A}\right)^2 \geq \left(1 + \frac{F_0 \cos \alpha}{f_1 A}\right)^2, \tag{10}$$

there is $\left(1 - \frac{F_0 \cos \gamma}{A}\right)^2 - \left(\frac{F_0 \cos \beta}{f_1 A}\right)^2 \geq \left(1 + \frac{F_0 \cos \alpha}{f_1 A}\right)^2 \geq 1$.

For the above equation, when $\cos \beta = 0$, $\cos \gamma = 0$, and $\cos \alpha = 0$ at the same time, then the left could be equal to the right. However, $\cos^2 \alpha + \cos^2 \beta + \cos^2 \gamma = 1$, and so $\cos \alpha$, $\cos \beta$, and $\cos \gamma$ cannot be all zero simultaneously. Hence, the supposition is not tenable. Therefore, there is $f^* < f_1$.

When the vibration force projects are in the second and the fourth quadrants of the xz plane, the model is shown in Figure 6.

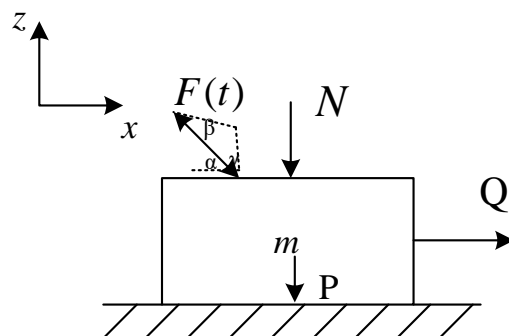


Figure 6. Vibration force projects in the second and the fourth quadrants.

Assume $|\cos \alpha| = i, |\cos \beta| = j, |\cos \gamma| = k$ and $i > 0, j \geq 0, k > 0$, there is,

$$(Q_{min} - F_0i)^2 + (F_0j)^2 = (f_1(N + mg - F_0k))^2. \tag{11}$$

Substituting $N + mg = A$ into the above equation, there is

$$f_1^* = f_1 \left(\sqrt{\left(1 - \frac{F_0k}{A}\right)^2 - \left(\frac{F_0j}{f_1A}\right)^2} + \frac{F_0i}{f_1A} \right), \tag{12}$$

where f_1^* is the effective coefficient of the friction when the vibration force project is in the second quadrant. Meanwhile, when the vibration force project is in the fourth quadrant, there is

$$(Q_{min} + F_0i)^2 + (F_0j)^2 = (f_1(N + mg + F_0k))^2, \tag{13}$$

where Q_{min} is the minimum force to move the material.

Simplifying the above expression yields

$$f_2^* = f_1 \left(\sqrt{\left(1 + \frac{F_0k}{A}\right)^2 - \left(\frac{F_0j}{f_1A}\right)^2} - \frac{F_0i}{f_1A} \right), \tag{14}$$

where f_2^* is the effective coefficient of friction when the vibration force project is in the fourth quadrant.

Hence, the effective friction coefficient f^* should be the minimum of the above, that is, $f^* = \min(f_1^*, f_2^*)$.

Suppose $\frac{i}{k} < f_1, \frac{F_0i}{f_1A} < \frac{F_0k}{A}, \left(1 - \frac{F_0i}{f_1A}\right)^2 > \left(1 - \frac{F_0k}{A}\right)^2 \geq \left(1 - \frac{F_0k}{A}\right)^2 - \left(\frac{F_0j}{f_1A}\right)^2$, there is

$$f_1^* = f_1 \left(\sqrt{\left(1 - \frac{F_0k}{A}\right)^2 - \left(\frac{F_0j}{f_1A}\right)^2} + \frac{F_0i}{f_1A} \right) < f_1. \tag{15}$$

Suppose $\frac{i}{k} > f_1, \frac{F_0i}{f_1A} > \frac{F_0k}{A}, \left(1 + \frac{F_0i}{f_1A}\right)^2 > \left(1 + \frac{F_0k}{A}\right)^2 \geq \left(1 + \frac{F_0k}{A}\right)^2 - \left(\frac{F_0j}{f_1A}\right)^2$, there is

$$f_1^* = f_1 \left(\sqrt{\left(1 + \frac{F_0k}{A}\right)^2 - \left(\frac{F_0j}{f_1A}\right)^2} - \frac{F_0i}{f_1A} \right) < f_1. \tag{16}$$

When $\frac{i}{k} = f_1$ and $j \neq 0$, there is $f_1^* < f_1, f_2^* < f_1$; when $\frac{i}{k} = f_1$ and $j = 0$, there is $f_1^* = f_2^* = f_1$.

To sum up, the results show that when $\frac{i}{k} = f_1$ and $j = 0$, there is $f^* = \min(f_1^*, f_2^*) = f_1$. Otherwise, there is $f^* < f_1$ always.

4. Negative Gradient of the Effective Friction Coefficient

In addition, the negative gradient η of the effective friction coefficient is discussed in this paper. The negative gradient has a critical effect on the ratio of the effective friction coefficient to the friction coefficient. Suppose $|\cos \alpha| = i, |\cos \beta| = j, |\cos \gamma| = k, \rho = \frac{F_0}{A}$. When $i \geq 0, j > 0, k > 0$ (in the first coordination), there is $1 - \rho k > 0$.

$$\eta = 1 - \frac{f^*}{f_1} = 1 - (|1 - \rho k| - \frac{\rho i}{f_1}) = \rho \sqrt{1 - i^2} + \frac{\rho i}{f_1} \tag{17}$$

and $i = \frac{1}{\sqrt{1+f_1^2}}, \eta'|_i = 0; \eta$ obtains the max value.

By deriving Equation (17), there is

$$\eta'|_i = -\rho\left(\frac{i}{\sqrt{1-i^2}} - \frac{1}{f_1}\right) \tag{18}$$

According to the values shown in Figure 7, there is no negative gradient at the $f_1 = 0$ stage. The curve is absolutely smooth, and the negative gradient η is always zero in this stage. When $f_1 = 0.1$, η is increased with ρ immediately, and the curve is much steeper. With the increase in f_1 , η will be stable gradually. When $f_1 = 1$, η will be flat.

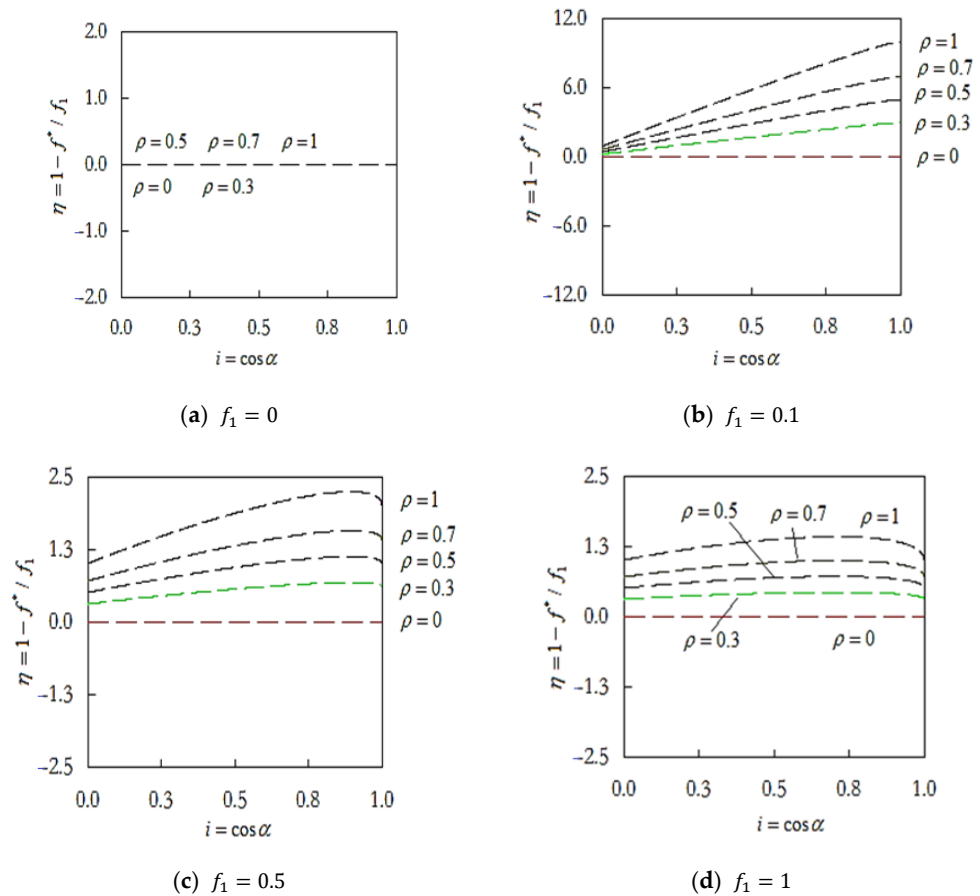


Figure 7. The negative gradient of the effective friction coefficient η .

According to $\begin{cases} i^2 + k^2 = 1 \\ i/k = f_1 \\ j = 0 \end{cases}$, there is

$$\begin{cases} i = \frac{f_1}{\sqrt{1+f_1^2}} \\ k = \frac{1}{\sqrt{1+f_1^2}} \\ j = 0 \end{cases} \tag{19}$$

Then, there is

$$\eta = 1 - \frac{f^*}{f_1} = \begin{cases} 1 - \left(1 - \rho k + \frac{\rho i}{f_1}\right), i/k < f_1 \\ 1 - \left(1 + \rho k - \frac{\rho i}{f_1}\right), i/k \geq f_1 \end{cases} = \left| \rho \sqrt{1-i^2} - \frac{\rho i}{f_1} \right| \tag{20}$$

$$\eta'|_i = \begin{cases} -\rho\left(\frac{i}{\sqrt{1-i^2}} + \frac{1}{f_1}\right), & 0 \leq i < \frac{f_1}{\sqrt{1+f_1^2}} \\ \rho\left(\frac{i}{\sqrt{1-i^2}} + \frac{1}{f_1}\right), & i = \frac{f_1}{\sqrt{1+f_1^2}} \end{cases} \quad (21)$$

To sum up, according to the values shown in Figure 8, there is no negative gradient in the stage of $f_1 = 0$. Obviously, there is no friction in this stage; η is always zero with increasing ρ . When $f_1 = 0.1$, η increases with ρ obviously, and then the curve will be steeper. When $f_1 = 0.5$, η decreases with ρ and decays to zero first, but then η increases with ρ gradually. In conclusion, the negative gradient of effective friction has a critical effect on friction. It was shown that the changes in the negative gradient of the effective friction coefficient changed the effective friction coefficient under the arbitrary time-varying external forces, which consequently reduced the friction. From a tribological perspective, the negative gradient of the effective friction coefficient plays a great role in the course of vibration affection on the friction. The rules concerning the negative gradient of the effective friction coefficient resulted in an effective friction coefficient, especially under the arbitrary time-varying external forces.

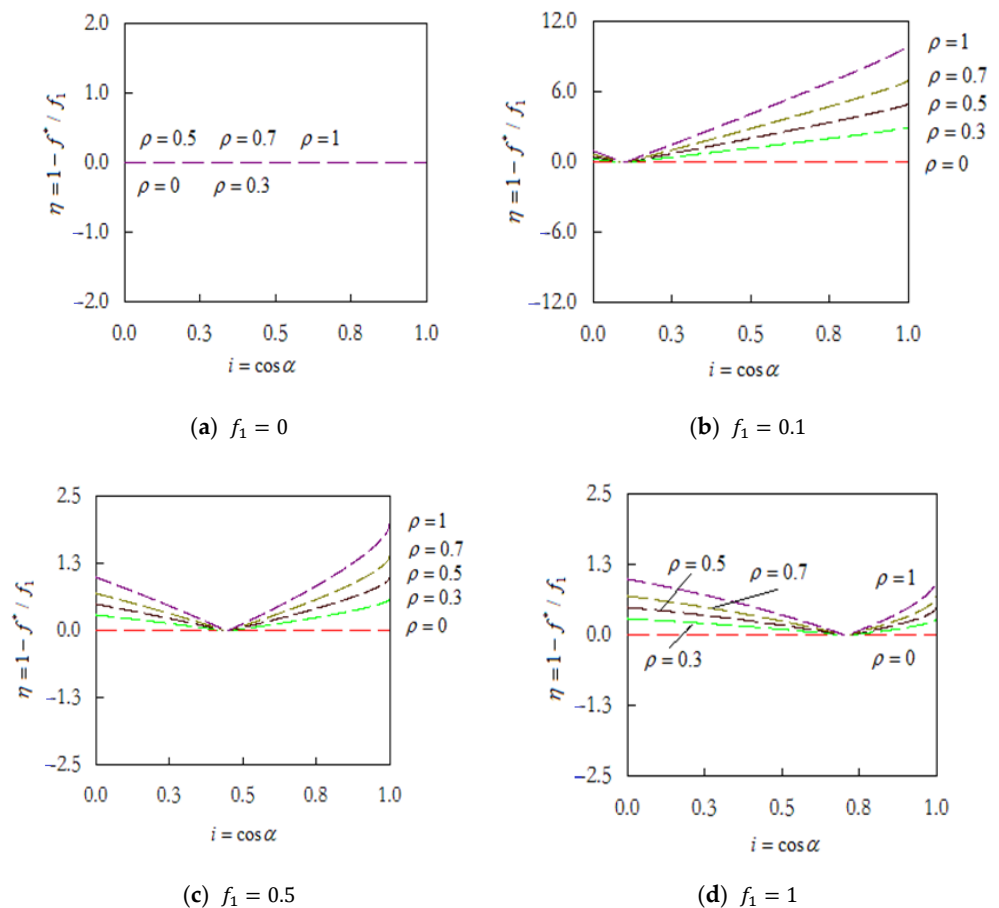


Figure 8. The negative gradient of effective friction coefficient η .

5. Conclusions

In conclusion, this paper investigated the effective coefficient of friction under arbitrary time-varying external forces. The results show the relationship of the effective friction coefficient and the negative gradient of friction.

(1) When the vibration force direction projects are in the first and the third quadrants, the negative gradient η increases first, and then η will be stable gradually. When the vibration force direction projects are in the second and the fourth quadrants, η decreases but then increases gradually.

(2) From a tribological perspective, the negative gradient of the effective friction coefficient plays a great role in the course of vibration affection on the friction. The changes in the negative gradient of the effective friction coefficient resulted in an effective friction coefficient, especially under the arbitrary time-varying external forces. The effective friction coefficient was closely related to vibration properties and the influence and control on vibration systems with friction.

(3) It is shown that the numerical and analytical results of the rules concerning the negative gradient of the effective friction coefficient change the effective friction coefficient under the arbitrary time-varying external forces, which consequently reduce the friction in vibration.

Author Contributions: Q.W.: software, writing the original draft, investigation. Y.T.: formulation, approach, review and editing, supervision, formal analysis. L.X.: validation. B.W.: validation. All authors have read and agreed to the published version of the manuscript.

Funding: This research has been supported by the National Natural Science Foundation of China NNSFC (Grant, No. 51305069).

Data Availability Statement: Some data, models, or code generated or used during the study are available from the corresponding author by request.

Conflicts of Interest: The authors declare no conflict of interest.

References

- Pérez-Aracil, J.; Camacho-Gómez, C.; Pereira, E.; Vaziri, V.; Aphale, S.S.; Salcedo-Sanz, S. Eliminating Stick-Slip Vibrations in Drill-Strings with a Dual-Loop Control Strategy Optimised by the CRO-SL Algorithm. *Mathematics* **2021**, *9*, 1526. [\[CrossRef\]](#)
- Sun, X.Q.; Wang, T.; Zhang, R.L.; Gu, F.S.; Ball, A.D. Numerical Modelling of Vibration Responses of Helical Gears under Progressive Tooth Wear for Condition Monitoring. *Mathematics* **2021**, *9*, 213. [\[CrossRef\]](#)
- Wu, J.T.; Yang, Y.; Yang, X.K.; Cheng, J.S. Fault feature analysis of cracked gear based on LOD and analytical-FE method. *Mech. Syst. Signal Pr.* **2018**, *98*, 951–967. [\[CrossRef\]](#)
- Sugiura, J.; Jones, S. Real-time stick-slip and vibration detection for 8 1/2"-hole-size rotary steerable tools in deeper wells and more aggressive drilling. In Proceedings of the AADE National Technical Conference, Houston, TX, USA, 10–12 April 2007.
- Robnett, E.; Hood, J.; Heisig, G.; Macpherson, J. Analysis of the stick-slip phenomenon using downhole drill string rotation data. In Proceedings of the SPE/IADC Drilling Conference, Amsterdam, The Netherlands, 9–11 March 1999.
- Baradaran-Nia, M.; Afizadeh, G.; Khanmohammadi, S.; Azar, B.F. Optimal sliding mode control of single degree-of-freedom hysteretic structural system. *Commun. Nonlinear Sci. Numer. Simul.* **2012**, *17*, 4455–4466. [\[CrossRef\]](#)
- Fu, X.; Ai, H.; Li, C. Repetitive Learning Sliding Mode Stabilization Control for a Flexible-Base, Flexible-Link and Flexible-Joint Space Robot Capturing a Satellite. *Appl. Sci.* **2021**, *11*, 8077. [\[CrossRef\]](#)
- Kumar, V.C.; Hutchings, I.M. Reduction of the sliding friction of metals by the application of longitudinal or transverse ultrasonic vibration. *Tribol. Int.* **2004**, *37*, 833–840. [\[CrossRef\]](#)
- Adachi, K.; Kato, K.; Sasatani, Y. The micro-mechanism of friction drive with ultrasonic wave. *Wear* **1996**, *194*, 137–142. [\[CrossRef\]](#)
- Tucker, W.; Wang, C. On the effective control of torsional vibrations in drilling systems. *J. Sound Vib.* **1999**, *224*, 101–122. [\[CrossRef\]](#)
- Carducci, G.; Giannoccaro, N.I.; Messina, A.; Rollo, G. Identification of viscous friction coefficients for a pneumatic system model using optimization methods. *Math. Comput. Simul.* **2006**, *71*, 385–394. [\[CrossRef\]](#)
- Tsai, C.C.; Tseng, C.H. The effect of friction reduction in the presence of in-plane vibrations. *Arch. Appl. Mech.* **2006**, *75*, 164–176. [\[CrossRef\]](#)
- Bao, H.; Huang, W.; Lu, F. Investigation of engagement characteristics of a multi-disc wet friction clutch. *Tribol. Int.* **2021**, *159*, 106940.
- Jia, S.H. The effective friction coefficient under the vibration. *J. Tsinghua Univ.* **1959**, *5*, 165–170.
- Jin, X.; Xu, H.; Wang, Y.; Huang, Z. Approximately analytical procedure to evaluate random stick-slip vibration of Duffing system including dry friction. *J. Sound Vib.* **2019**, *443*, 520–536. [\[CrossRef\]](#)
- Marino, L.; Cicirello, A. Experimental investigation of a single-degree-of-freedom system with Coulomb friction. *Nonlinear Dyn.* **2020**, *99*, 1781–1799. [\[CrossRef\]](#)
- Wang, D.W.; Mo, J.L.; Wang, Z.G.; Chen, G.X.; Ouyang, H.; Zhou, Z.R. Numerical study of friction-induced vibration and noise on groove-textured surface. *Tribol. Int.* **2013**, *64*, 1–7. [\[CrossRef\]](#)
- Wang, X.C.; Huang, B.; Wang, R.L.; Mo, J.L.; Ouyang, H. Friction-induced stick-slip vibration and its experimental validation. *Mech. Syst. Signal Process.* **2020**, *142*, 106705. [\[CrossRef\]](#)
- Sun, G.D.; Zhu, H.; Ding, C. Using Recurrence Plots for Stability Analysis of Ring-on-Disc Tribopairs. *Ind. Lubr. Tribol.* **2019**, *71*, 532–539. [\[CrossRef\]](#)

20. Sun, G.D.; Zhu, H.; Ding, C.; Jiang, Y.; Wei, C.L. On the Boundedness of Running-In Attractors Based on Recurrence Plot and Recurrence Qualification Analysis. *Friction* **2019**, *7*, 432–443. [[CrossRef](#)]
21. Liu, Y.; Pavlovskaja, E.; Hendry, D.; Wiercigroch, M. Vibro-impact responses of capsule system with various friction models. *Int. J. Mech. Sci.* **2013**, *72*, 39–54. [[CrossRef](#)]
22. Marques, F.; Flores, P.; Pimenta Claro, J.C.; Lankarani, H.M. A survey and comparison of several friction force models for dynamic analysis of multibody mechanical systems. *Nonlinear Dyn.* **2016**, *86*, 1407–1443. [[CrossRef](#)]
23. Mostaghel, N. A non-standard analysis approach to systems involving friction. *J. Sound Vib.* **2005**, *284*, 583–595. [[CrossRef](#)]
24. Rusinek, R.; Wiercigroch, M.; Wahi, P. Modelling of frictional chatter in metal cutting. *Int. J. Mech. Sci.* **2014**, *89*, 167–176. [[CrossRef](#)]
25. Saha, A.; Wiercigroch, M.; Jankowski, K.; Wahi, P.; Stefański, A. Investigation of two different friction models from the perspective of friction-induced vibrations. *Tribol. Int.* **2015**, *90*, 185–197. [[CrossRef](#)]
26. Yan, Y.; Liu, G.; Wiercigroch, M.; Xu, J. Safety estimation for a new model of regenerative and frictional cutting dynamics. *Int. J. Mech. Sci.* **2021**, *201*, 106468. [[CrossRef](#)]
27. Yoo, S.S.; Kim, D.E. Effects of vibration frequency and amplitude on friction reduction and wear characteristics of silicon. *Tribol. Int.* **2016**, *16*, 198–206. [[CrossRef](#)]
28. Safaei, B. Frequency-dependent damped vibrations of multifunctional foam plates sandwiched and integrated by composite faces. *Eur. Phys. J. Plus* **2021**, *136*, 646. [[CrossRef](#)]
29. Duc, D.H.; Thom, D.V.; Cong, P.H.; Minh, P.V.; Nguyen, N.X. Vibration and static buckling behavior of variable thickness flexoelectric nanoplates. *Mech. Based Des. Struct. Mach.* **2022**, *8*, 1–29. [[CrossRef](#)]
30. Dung, N.T.; Van Ke, T.; Huyen, T.T.H.; Van Minh, P. Nonlinear static bending analysis of microplates resting on imperfect two-parameter elastic foundations using modified couple stress theory. *Comptes Rendus Mec.* **2022**, *350*, 121–141. [[CrossRef](#)]
31. Tho, N.C.; Ta, N.T.; Thom, D.V. New Numerical Results from Simulations of Beams and Space Frame Systems with a Tuned Mass Damper. *Materials* **2019**, *12*, 1329. [[CrossRef](#)] [[PubMed](#)]
32. Han, S.Y.; Narasimhan, M.N.L.; Kennedy, T.C. Finite crack propagation in a micropolar elastic solid. *KSME J.* **1989**, *3*, 103. [[CrossRef](#)]
33. Kumar, R.; Singh, R.; Chadha, T.K. Eigen value approach to second dynamic problem of micropolar elastic solid. *Indian J. Pure Appl. Math.* **2003**, *34*, 743–754.
34. Tuan, L.T.; Dung, N.T.; Van Thom, D.; Van Minh, P.; Zenkour, A.M. Propagation of non-stationary kinematic disturbances from a spherical cavity in the pseudo-elastic cosserat medium. *Eur. Phys. J. Plus* **2021**, *136*, 1199. [[CrossRef](#)]
35. Tran, T.T.; Tran, V.K.; Le, P.B.; Phung, V.M.; Do, V.T.; Nguyen, H.N. Forced vibration analysis of laminated composite shells reinforced with graphene nanoplatelets using finite element method. *Adv. Civ. Eng.* **2020**, *2020*, 1471037. [[CrossRef](#)]
36. Nam, V.H.; Nam, N.H.; Vinh, P.V.; Khoa, D.N.; Thom, D.V.; Minh, P.V. A new efficient modified first-order shear model for static bending and vibration behaviors of two-layer composite plate. *Adv. Civ. Eng.* **2019**, *2019*, 6814367. [[CrossRef](#)]
37. van Thom, D.; Duc, D.H.; van Minh, P.; Tung, N.S. Finite element modelling for free vibration response of cracked stiffened fgm plates. *Vietnam J. Sci. Technol.* **2020**, *58*, 119. [[CrossRef](#)]
38. Tho, N.C.; Thanh, N.T.; Tho, T.D.; van Minh, P.; Hoa, L.K. Modelling of the flexoelectric effect on rotating nanobeams with geometrical imperfection. *J. Braz. Soc. Mech. Sci. Eng.* **2021**, *43*, 510. [[CrossRef](#)]
39. Dung, N.T.; van Minh, P.; Hung, H.M.; Tien, D.M. The third-order shear deformation theory for modelling the static bending and dynamic responses of piezoelectric bidirectional functionally graded plates. *Adv. Mater. Sci. Eng.* **2021**, *2021*, 5520240. [[CrossRef](#)]